New Generation of X-ray Reflection Models from Ionized Accretion Disks around Black Holes

Javier García

Harvard-Smithsonian Center for Astrophysics

The FERO Meeting
Finding Extreme Relativistic Objects
Krakow, 28th - 30th August 2014

August 29th, 2014

In Collaboration with:

- **J. McClintock, J. Steiner, L. Brenneman, R. Narayan**
  Harvard-Smithsonian Center for Astrophysics
- **T. Dauser, J. Wilms, W. Eikmann**
  Dr. Karl Remeis-Observatory, Bamberg, Germany
- **T.R. Kallman**
  NASA Goddard Space Flight Center
- **C.S. Reynolds, A. Lohfink, F. Tombesi**
  Department of Astronomy, University of Maryland

Motivation

Big Picture: To measure the spin of Black Holes

- Two effective methods:
  - The continuum-method (Soft/Thermal state, see McClintock+13)
  - Fe-line method (Hard/PL state, see Reynolds+13)

X-ray reflection models are the cornerstone of the Fe-line method

Not so Big Picture: X-ray reflection is present in nearly every spectra from accreting sources

- Galactic Black Holes (Miller+12)
- Active Galactic Nuclei (Reynolds+13)
- Neutron Stars (Cackett+12)
- Ultra Compact X-ray Binaries (Gilfanov10)
- Supersoft X-ray sources (Suleimanov+03)
- X-ray Pulsars (Ballantyne+12)

X-ray Reflection from Accretion Disks: XILLVER

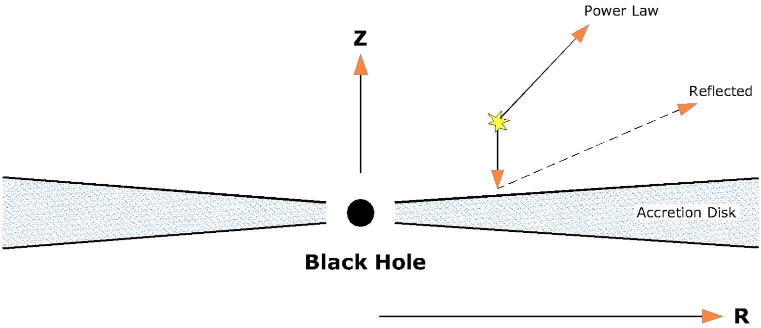

- The accretion disk is illuminated by a source of X-rays
- Radiation is reprocessed in an optically-thick material
- The 'reflected' spectrum contains both emission and absorption features from ions in the gas
- This component is observed in nearly all accreting sources (e.g. AGNs, GBHs, NS).

XILLVER in a Nutshell

In any photoionized plasma, one needs to solve (at least) 3 basic equations: **Level Populations**, **Energy,** and **Radiation Transfer**

- Incident photons excite and/or ionize atoms in the gas
- The gas is heated by photo-absorption or scattering of photons by cold electrons
- Cooling is achieved by both continuum and line emission
- Equilibrium is reached at a particular temperature where heating = cooling
- Therefore, the gas **temperature** needs to be calculated self-consistently, and the **ionization balance** is determined by the strength and shape of the **radiation field**
- Complex emergent spectrum:
    - Absorption: continuous (photoelectric); discrete (lines, resonances and edges)
    - Emission: continuous (thermal black-body, bremsstrahlung); discrete (fluorescence lines, radiative recombination continua)

XILLVER in a Nutshell

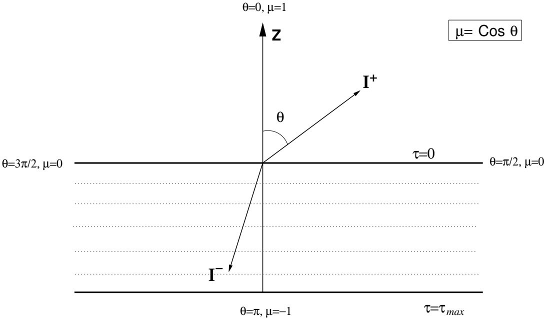

- Solve Radiation Transfer equation in 1D, plane-parallel geometry
- Solve ionization balance using XSTAR (Kallman+Bautista10)
- Calculations include the most recent and complete atomic data for K-shell transitions
- Compton scattering is included via a convolution kernel

XILLVER: $\log \xi = 2$, $\Gamma = 2$, $A_{\rm Fe} = 1$

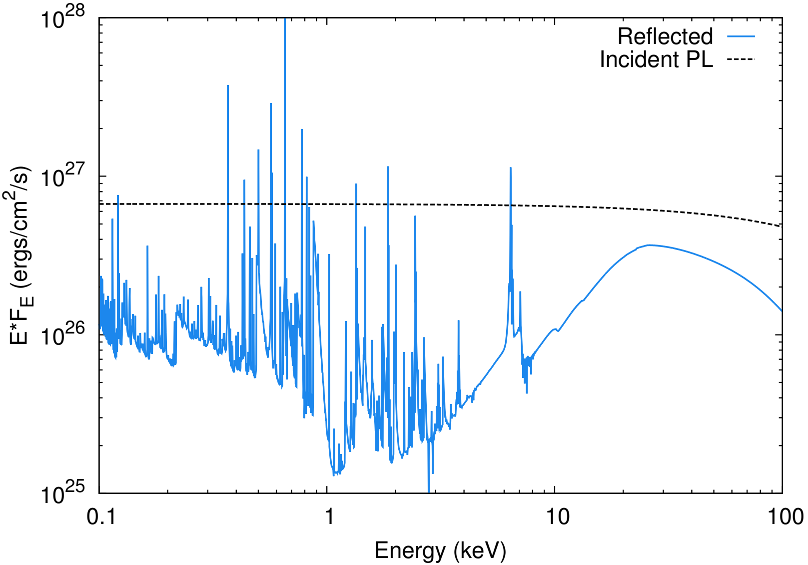

XILLVER: log $\xi = 2$, $\Gamma = 2$, $A_{\mathrm{Fe}} = 1$

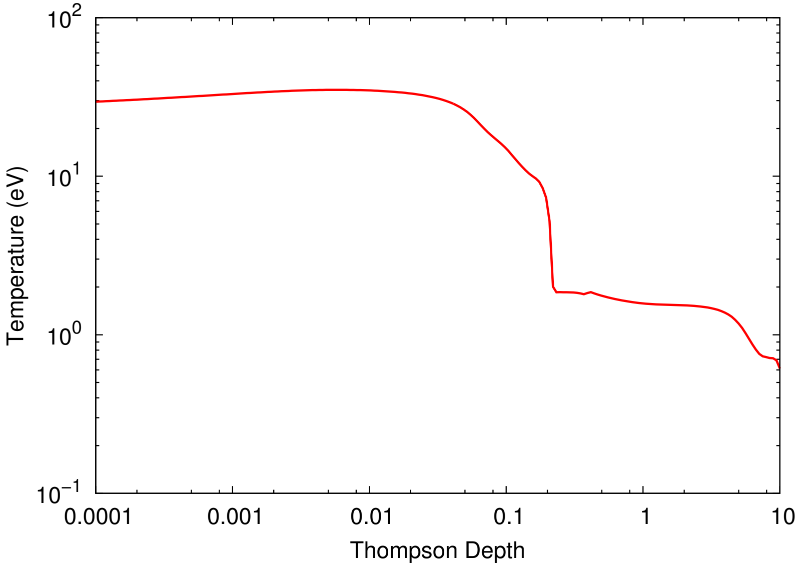

Ionization Balance

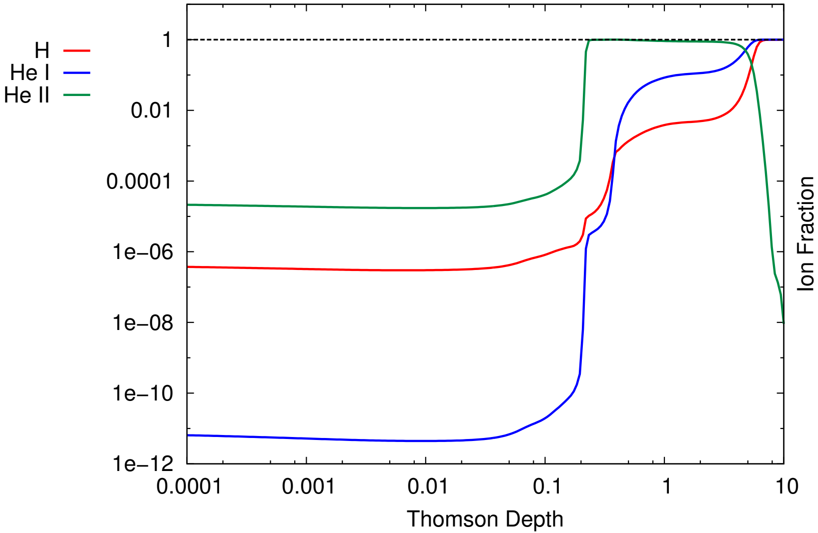

Ionization Balance

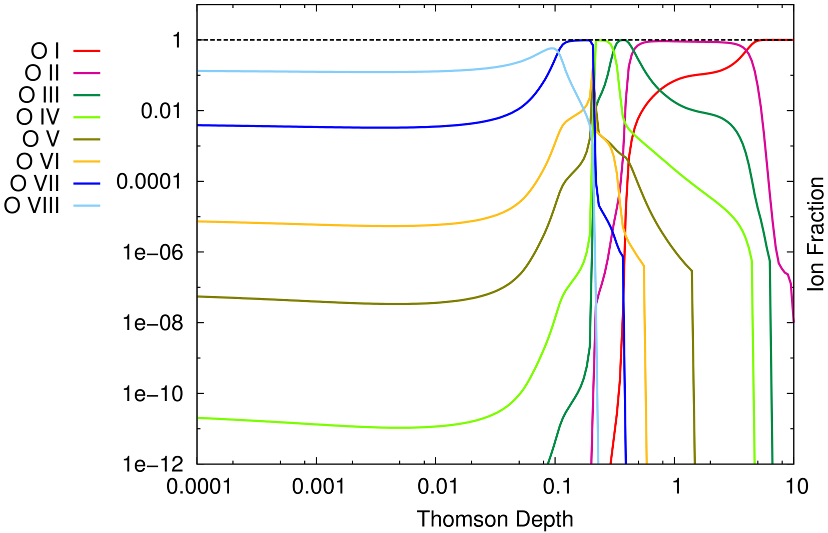

Ionization Balance

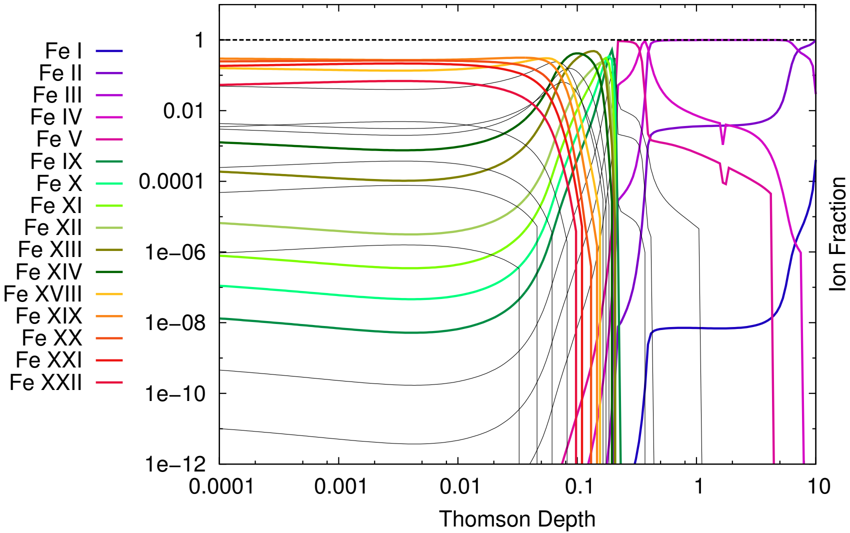

Variable Ionization Parameter ξ

Low- to high-ionization reflected spectra for $\Gamma = 2$ and solar abundances.

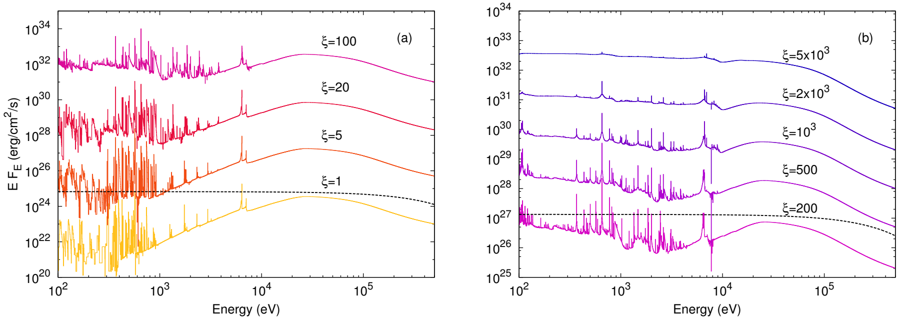

(García+13)

Variable Photon Index Γ

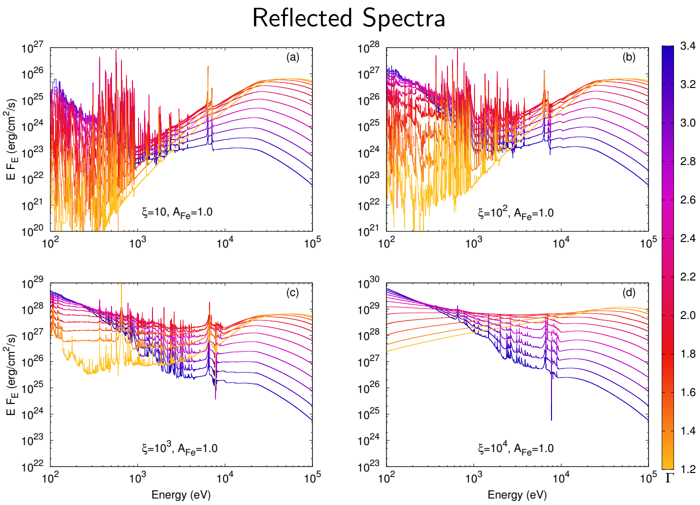

(García+13)

Variable Iron Abundance A_{Fe}

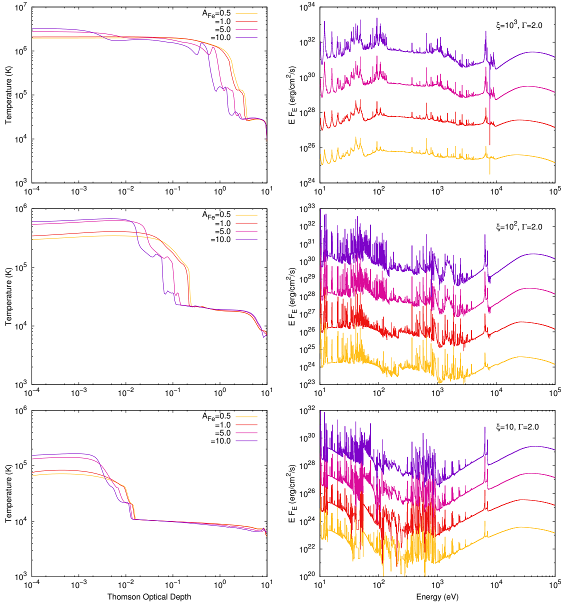

(García+13)

Emission lines from all the Fe ions in the $6 - 10$ keV energy range.
Red circles: Transitions with $A_r > 10^{13}$ s^{-1}.

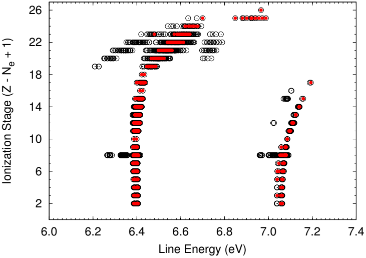

http://heasarc.gsfc.nasa.gov/uadb/

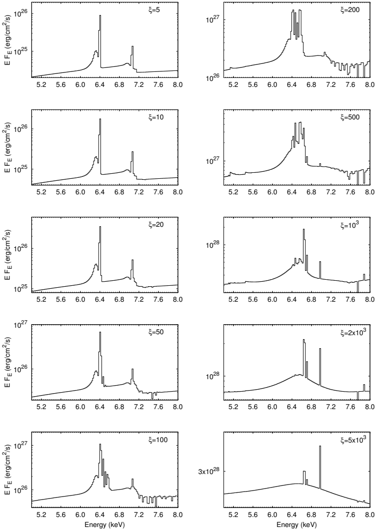

(Kallman+04, García+13)

Lower-Z elements

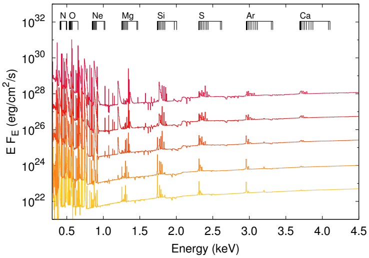

XILLVER spectra for $\Gamma = 3$ and solar abundances.
Ionization increases upward in each Figure.

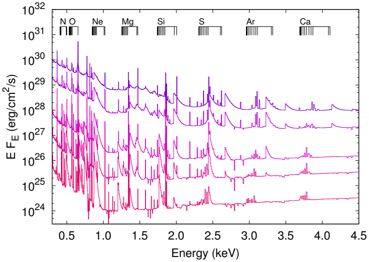

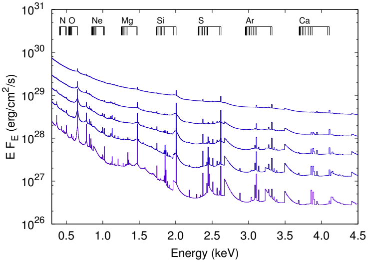

(García+13)

The Emission Angle: Reflection Spectrum

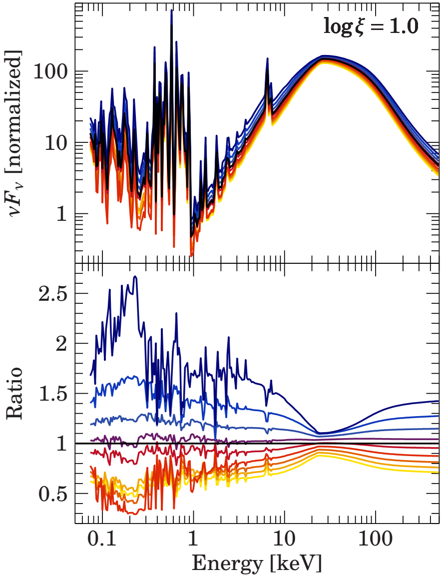

Reflection Spectra differ depending on the **Emission Angle**

However, common Convolution Models use **Angle Averaged Reflection Spectra**

Angular Effects

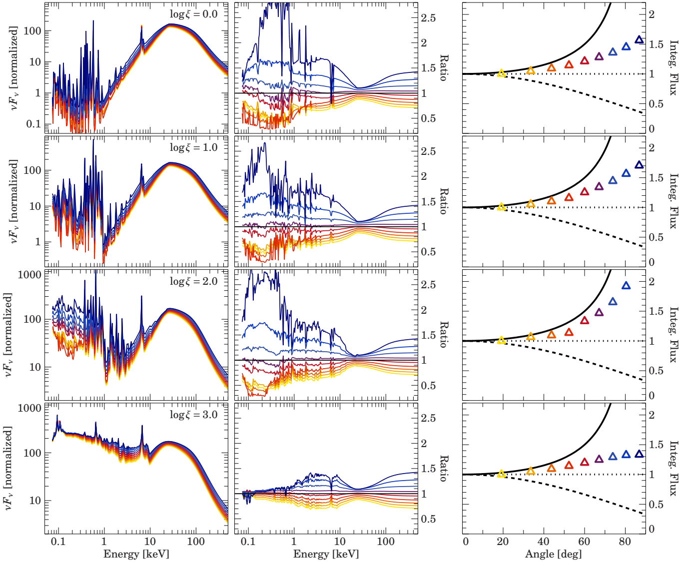

Angular Effects

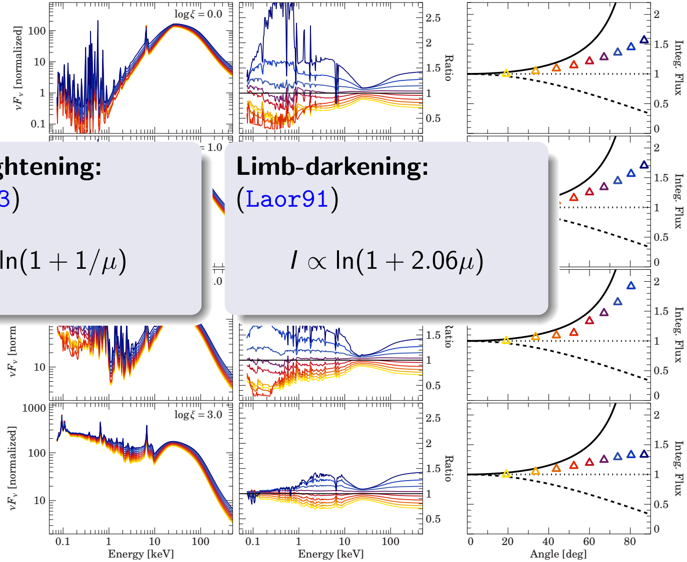

Limb-brightening:
(Haardt93)

$$I \propto \ln(1 + 1/\mu)$$

Limb-darkening:
(Laor91)

$$I \propto \ln(1 + 2.06\mu)$$

Angular Effects

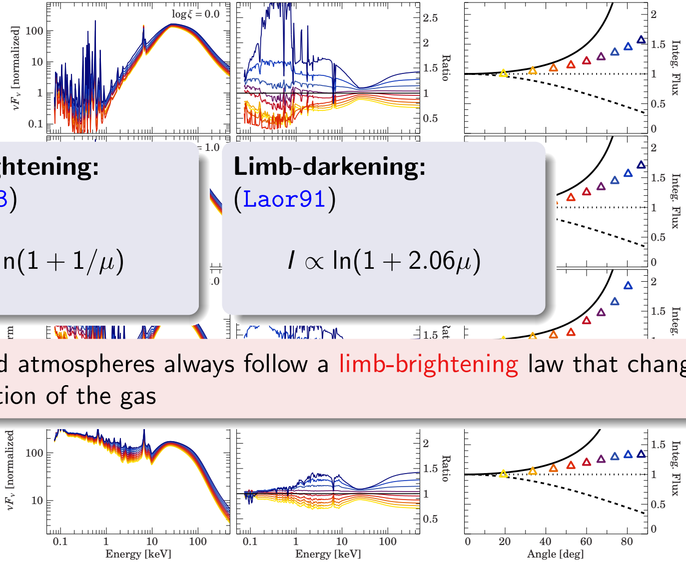

Limb-brightening:
(Haardt93)

$$I \propto \ln(1 + 1/\mu)$$

Limb-darkening:
(Laor91)

$$I \propto \ln(1 + 2.06\mu)$$

Illuminated atmospheres always follow a limb-brightening law that changes with the ionization of the gas

Modeling Relativistic Reflection: RELXILL

RELXILL: Relativistic reflection model that combines detailed reflection spectra from **xillver** (García & Kallman 2010), with the **relline** relativistic blurring code (Dauser et al. 2010).

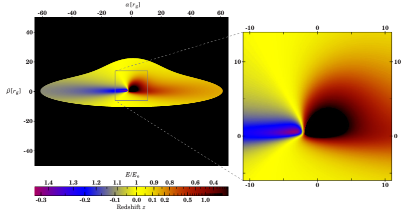

Model Parameters

a: Black hole spin, R_{in}: Disk's inner edge
i: Inclination, ϵ: Emissivity index
R_f: Reflection fraction, Γ: Power-law index
E_{cut}: High-energy cutoff, A_{Fe}: Fe abundance

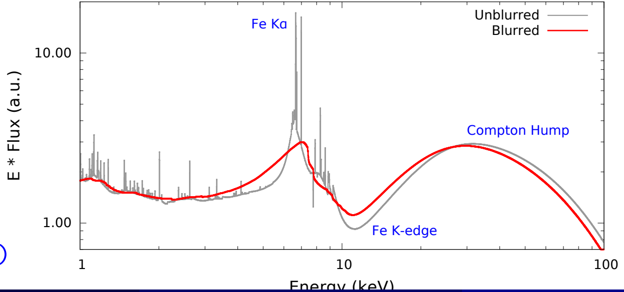

(García+14b)

Diagnostic potential: **black hole spin**

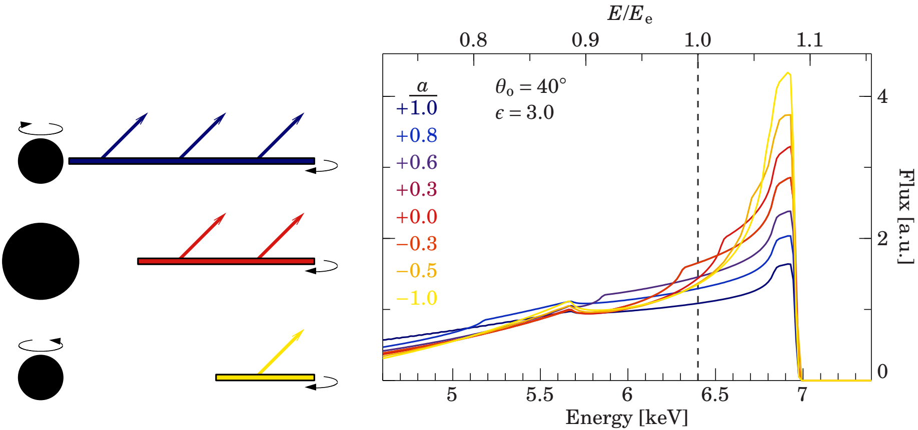

possible **Spin** values: $\mathbf{a} = -1 \ldots 1$

high Spin $\longrightarrow$ **broad line** (not always true, see later)

Diagnostic potential: **inclination**

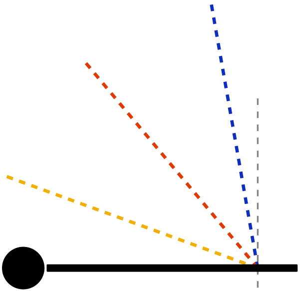

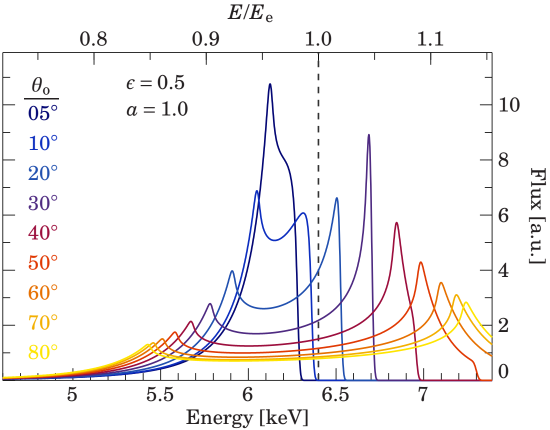

The Emission Angle: Relativistic Effects

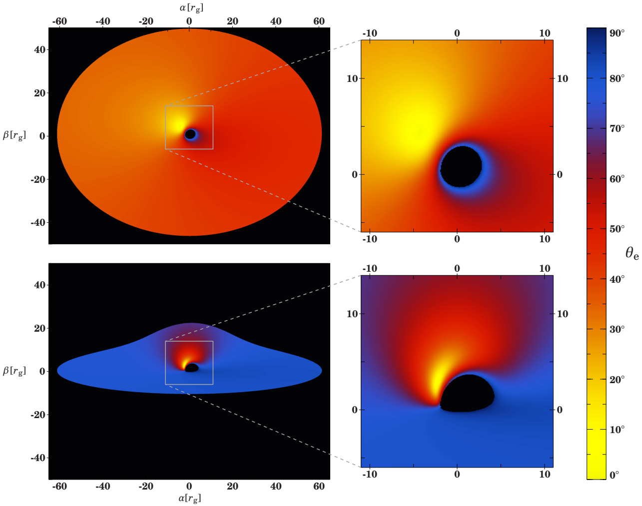

Relativistic blurring code RELLINE (Dauser+10).

The Emission Angle: Relativistic Reflection

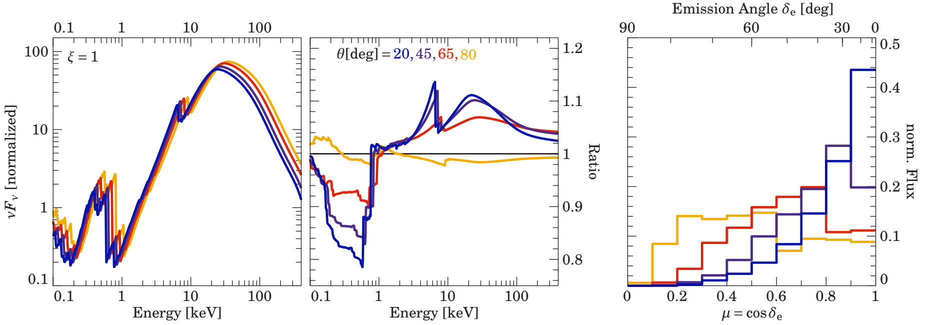

⇒ Differences up to 20% between the proper treatment and the angle-averaged model.

Note, **ALL reflection** codes (e.g., `reflionx` or `xillver`) convolved by **ANY relativistic** code (e.g., `kyconv`, `kerrconv`, or `relline`) are **angle-averaged**

The Emission Angle: Bias to the Angle Averaged Model

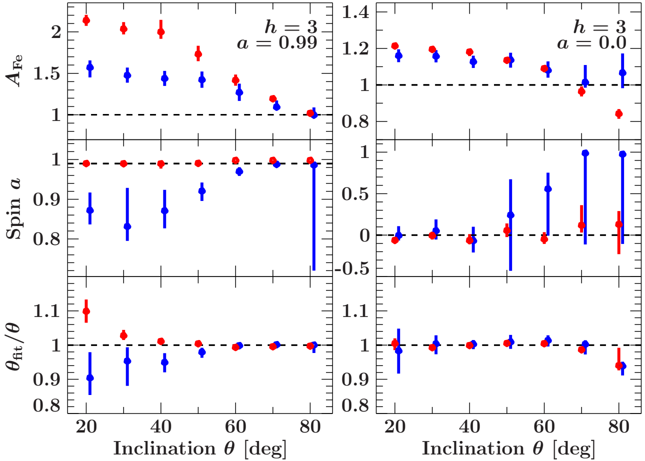

XMM-Newton sim., 100 ksec, flux similar to MCG−6-30-15 (neutral, ionized)

Bias: mainly iron abundance (up to a factor 2), but also spin and inclination (`García+Dauser+13, submitted`)

The new model `relxill`: Fit to Ark 120

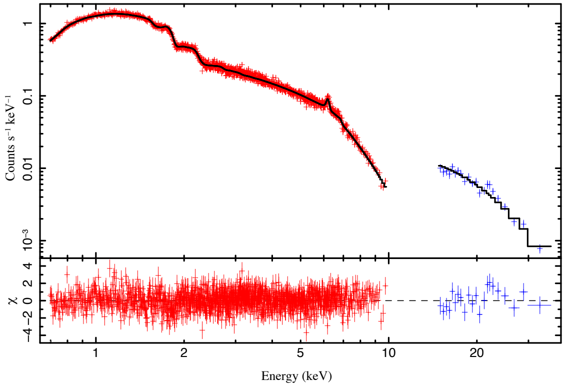

Par	Value
$q_{in} = q_{out}$	$4.8^{+1.8}_{1.1}$
a	$0.655^{+0.122}_{-0.126}$
i (deg)	$45.3^{+4.8}_{-2.4}$
R_{in} (ISCO)	1
R_{out} (ISCO)	400
z	0.0327
Γ	$2.17^{+0.02}_{-0.01}$
$\log \xi$	$0.84^{+0.24}_{-0.10}$
A_{Fe}	$1.78^{+0.39}_{-0.40}$
`angle_on`	1
$N(10^{-4})$	$2.07_{-0.2}$
$N(10^{-4})$	$0.14^{+0.07}_{-0.04}$

Suzaku spectrum of the Seyfert 1 galaxy Ark 120 (XIS,PIN). The solid line is the best-fit using the new `relxill` model. (`García+Dauser+14`)

The new model `relxill`: Fit to Ark 120

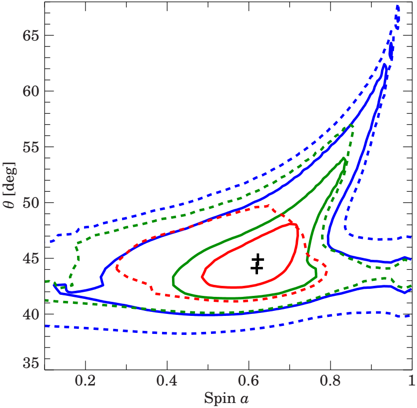

Contour plots of the **inclination** and **spin** a_* for 69% 90%, and 99% confidence levels.

Parameters are better constrained with the new angle-resolved model (solid lines), than with the angle-averaged version (dashed-lines). (`García+Dauser+14`)

RELXILL_LP: Lampost Geometry

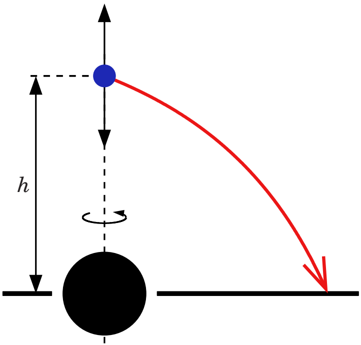

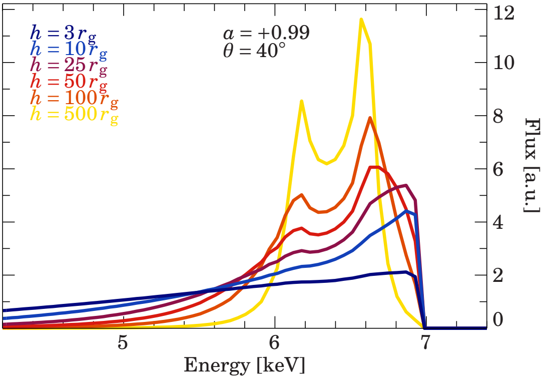

Probe the geometry and location of the Primary Source
→ **low height** implies **enhanced irradiation** of the **inner parts**

radially extended sources are also possible → **Jets**

Reflection Fraction in Lampost Geometry

$$R_f = \frac{F_{AD}}{F_\infty}$$

Fraction of the photons that reach the disk to those that reach infinity

$$R_f = ?$$

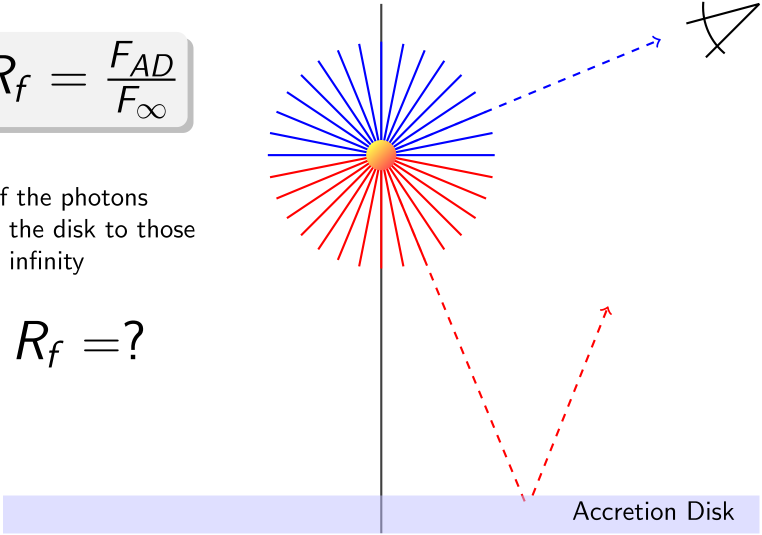

Reflection Fraction in Lampost Geometry

$$R_f = \frac{F_{AD}}{F_\infty}$$

Fraction of the photons that reach the disk to those that reach infinity

$$R_f = 1$$

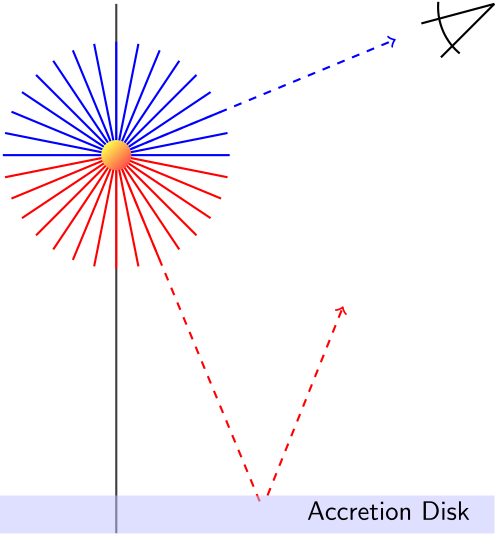

Reflection Fraction in Lampost Geometry

$$R_f = \frac{F_{AD}}{F_\infty}$$

Fraction of the photons that reach the disk to those that reach infinity

$$R_f < 1$$

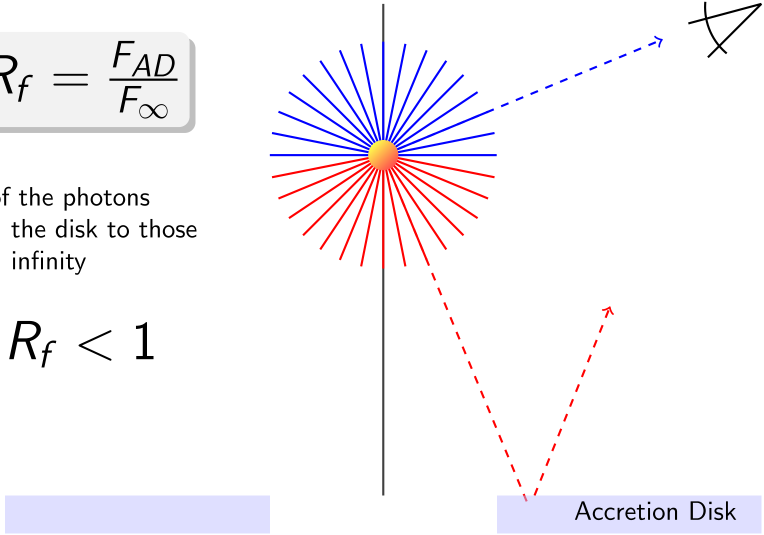

Reflection Fraction in Lampost Geometry

$$R_f = \frac{F_{AD}}{F_\infty}$$

Fraction of the photons that reach the disk to those that reach infinity

$R_f = ?$

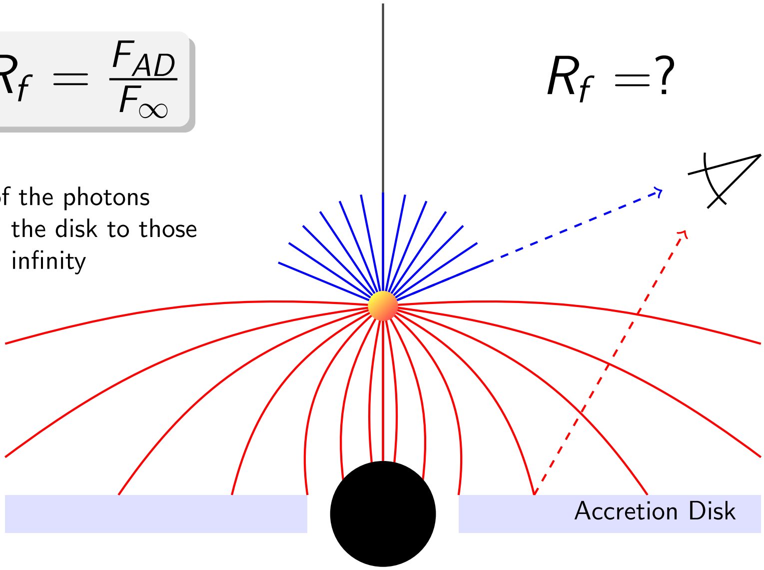

Reflection Fraction in Lampost Geometry

$$R_f = \frac{F_{AD}}{F_\infty}$$

$$R_f > 1$$

Fraction of the photons that reach the disk to those that reach infinity

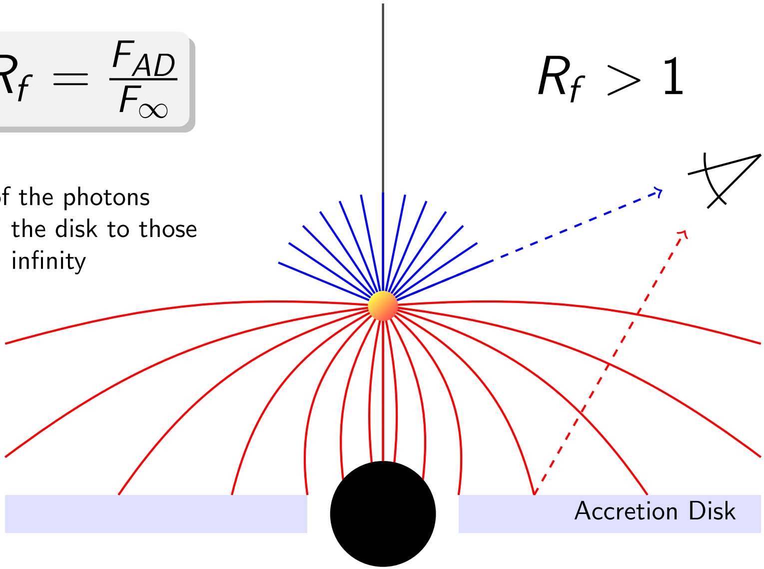

Reflection Fraction in Lampost Geometry

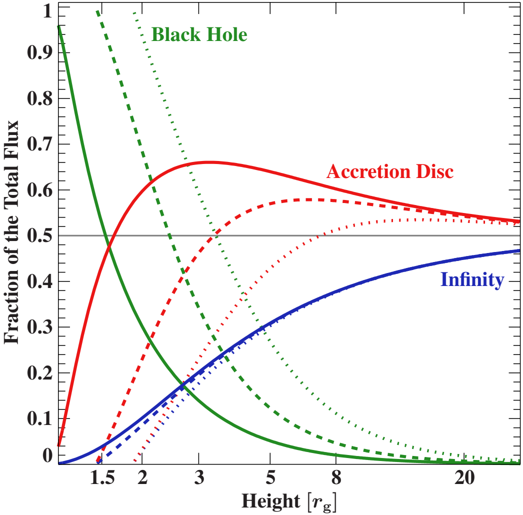

Stationary and isotropic radiating source on the axis of symmetry of the accretion flow, fractions are shown as a function of height of the primary source and for $a = 0.998$ (solid), $a = 0.9$ (dashed), and $a = 0.5$ (dotted lines).

Reflection Fraction from RELXILL

Main parameters that control R_f: BH spin a, inner radius r_{in}, and the height h of the X-ray source.

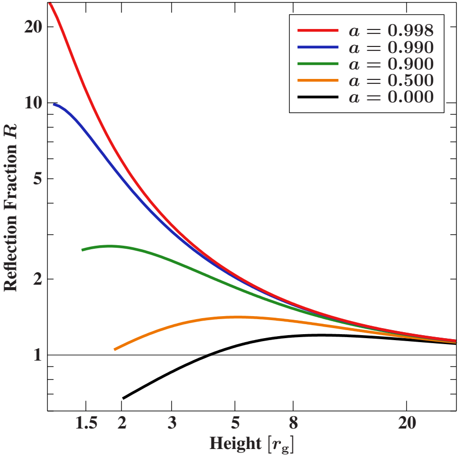

Maximum Reflection Fraction

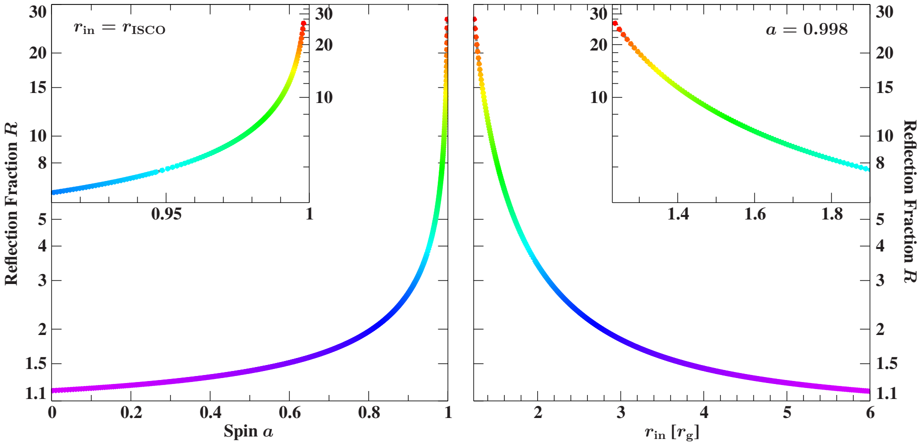

Maximum Reflection Fraction

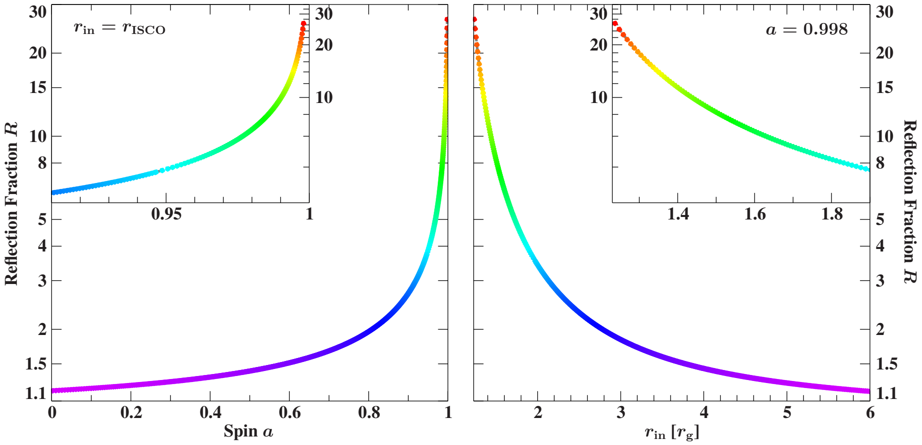

Unphysical solutions can be excluded!

Height for Maximum $R_f(max)$ versus spin

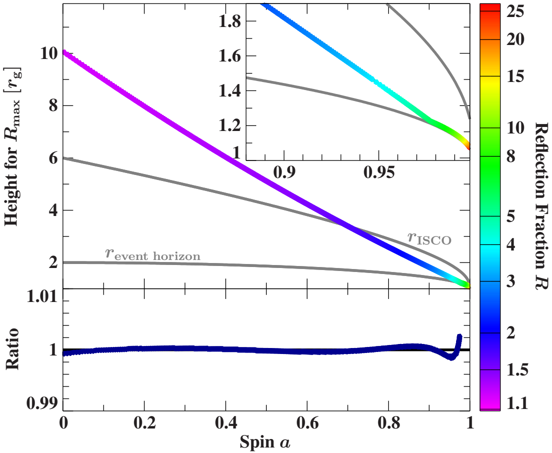

$$h_{R_{max}}(a) = (1.89a^2 - 10.86a + 10.07)\left(1 + \frac{9.41\times10^{-4}}{log(a)}\right), \text{ for } a < 0.975$$

$$h(R_{max}) = 1 + \sqrt{1 - a^2}, \text{ for } a > 0.975$$

Observational Implications

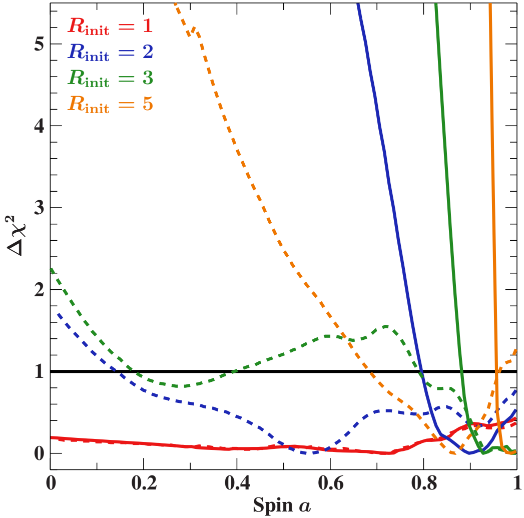

100 ks simulation of an AGN with XMM-Newton EPIC-pn. Model used is tbabs*relxill, with the emissivity index of 3, $a = 0.97$, $i = 30\,\mathrm{deg}$, $\Gamma = 2$, A_{Fe}, and $\xi = 100$ erg cm s^1.

Dashed lines: R_f allowed to be free.
Solid lines: R_f constrained to $R_f \leq R_{max}$

Observational Implications

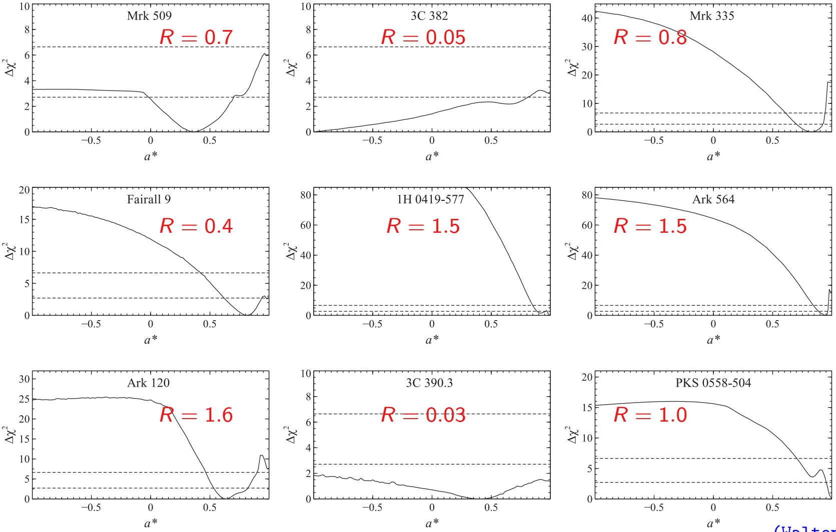

(Walton+13)

Observational Implications

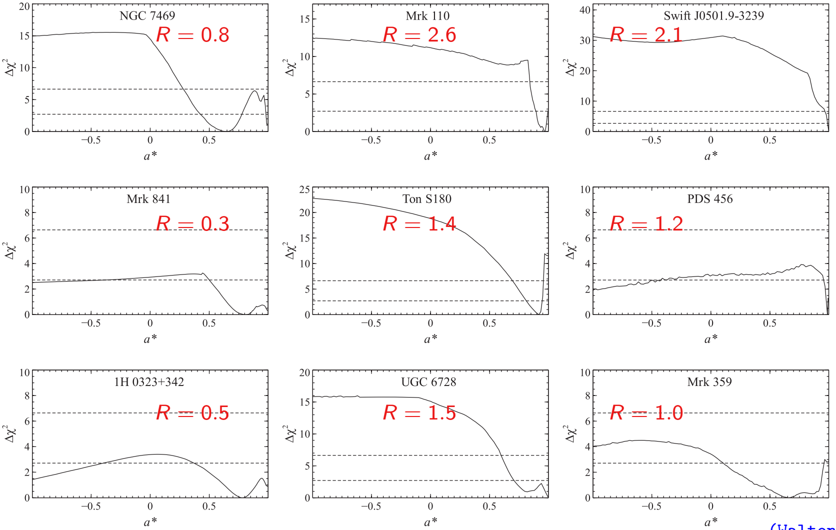

(Walton+13)

Observational Implications

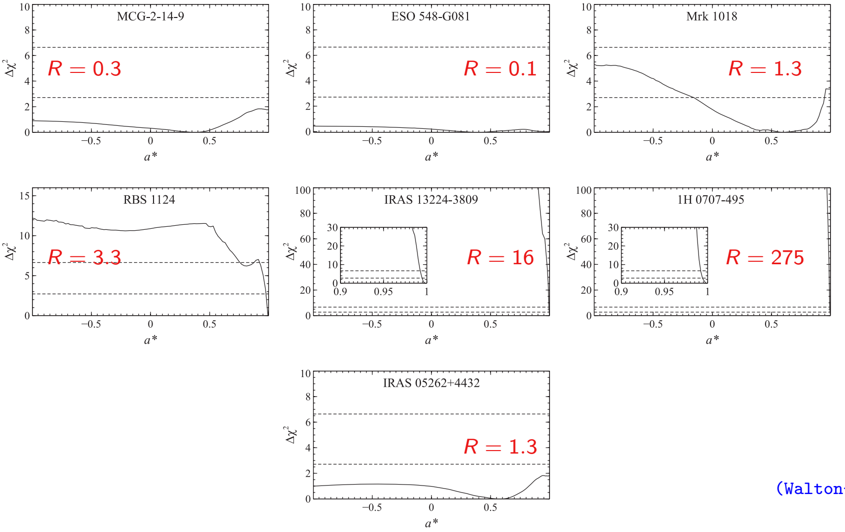

(Walton+13)

Observational Implications: Mrk 335

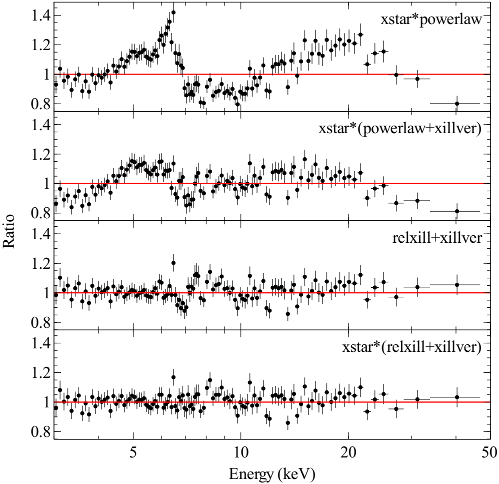

3 – 50 keV 100 ks *NuSTAR* observation of the AGN Mrk 335 in a very low flux state.

(Parker+14)

Observational Implications: Mrk 335

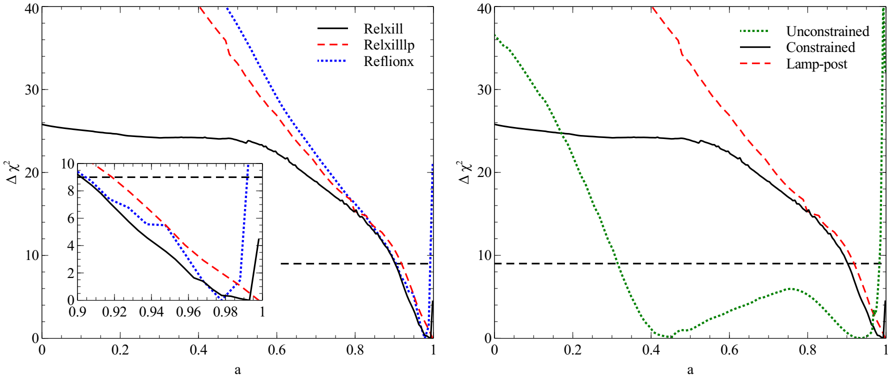

(Parker+14)

Observational Implications: Spin Distribution

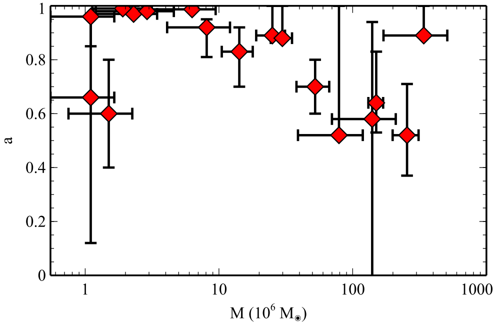

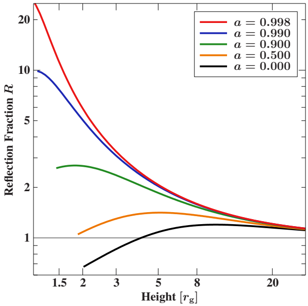

(Reynolds+13)

High-spin preference can be due to an observational bias

Summary: New Set of Reflection Models

Relativistically Blurred Reflection

http://www.sternwarte.uni-erlangen.de/research/relxill/

relxill: Broken PL emissivity

- q_{in}, q_{out}, R_{br}
- a_*, R_{in}, R_{out}, i
- $\Gamma, \xi, A_{\rm Fe}$
- $z, N,$ angleon

relxill_lp: Lampost

- h
- a_*, R_{in}, R_{out}, i
- $\Gamma, \xi, A_{\rm Fe}$
- $z, N,$ angleon

Pure Reflection

xillver: Library of 57600 spectra

- Photon index $1.2 \leq \Gamma \leq 3.4$
- Ionization parameter $1 \leq \xi \leq 10^4$
- Fe abundance $0.5 \leq A_{\rm Fe} \leq 10$
- Inclination $5^\circ \leq i \leq 85^\circ$
- High-Energy Cutoff (keV) $20 \leq E_c \leq 300$

Current and Future Developments

- **Reflected spectra to model GBHs (including thermal disk component).**
- **Relativistic reflection considering an ionization gradient in the radial direction.**
- **Hydrostatic atmospheres (e.g.** Rozanska+08, Nayakshin+00, Ballantyne+01**).**
- **Connection with GR-MHD simulations (e.g.** Schnittman+Krolik13**).**

Final Remarks

- Theory says spin should profoundly affect the behavior of accreting black holes, with potential implications on relevant problems such as relativistic jets power, galaxy evolution and high-energy physics acceleration.
- Broad Fe lines are a great tool in the black hole spin determination, with reflection modeling playing a mayor role. Current results suggest that reflection from accretion disks could be more complicated than what we thought.
- Black holes spins are currently being measured by either the Continuum Fitting or the Fe-line Fitting Methods. However, both methods need to be improved and brought into agreement.

Backup Slides

Ionization Gradients

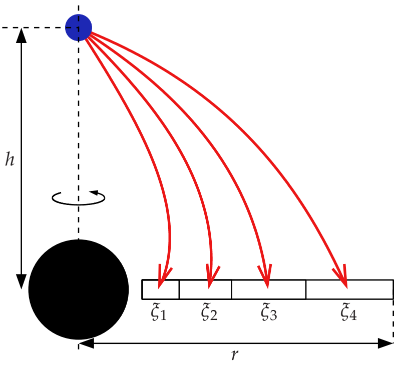

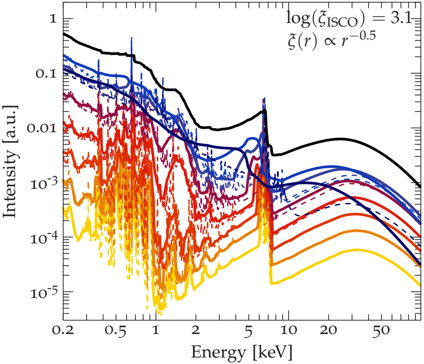

Ionization Gradients

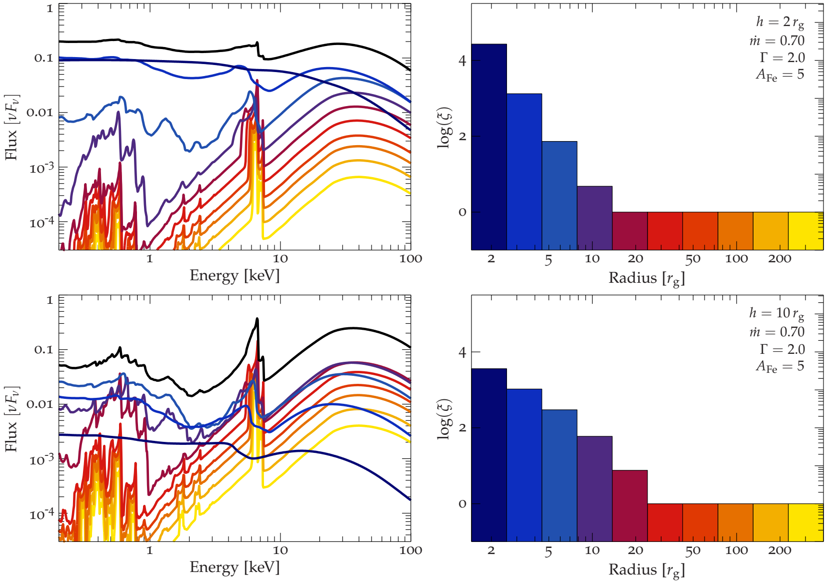

Final Remarks

- Theory says spin should profoundly affect the behavior of accreting black holes, with potential implications on relevant problems such as relativistic jets power, galaxy evolution and high-energy physics acceleration.
- Broad Fe lines are a great tool in the black hole spin determination, with reflection modeling playing a mayor role. Current results suggest that reflection from accretion disks could be more complicated than what we thought.
- Black holes spins are currently being measured by either the Continuum Fitting or the Fe-line Fitting Methods. However, both methods need to be improved and brought into agreement.

Comparison with other models

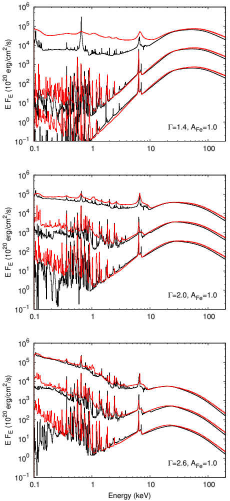

Reflected spectra from XILLVER and REFLIONX models (Ross+Fabian05)

- Good agreement in the Fe K line and edge positions.
- Fe Kα is stronger in XILLVER (affects $A_{\rm Fe}$)
- Lack of Fe Kβ and many lower-Z lines in REFLIONX due to the atomic data (may affect ξ)
- Best overall agreement for large Γ and low ξ
- Excess of flux in the soft-band always present in REFLIONX spectra

(García+13)

Equivalent Widths

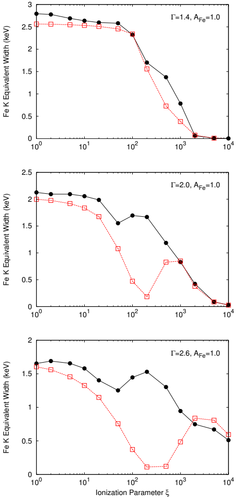

Equivalent widths for the Fe K emission

$$EW = \int_{5.5 \text{ keV}}^{7.2 \text{ keV}} \frac{F(E) - F_c(E)}{F_c(E)} dE$$

- For low-ξ XILLVER EWs are large due to the Fe Kβ emission
- Good agreement in models with high-ξ
- Larger discrepancies for $10^2 \lesssim \xi \lesssim 10^3$: in REFLIONX the Fe K emission is assumed to be suppressed by Resonant Auger Destruction
- XILLVER does not include resonant absorption. Line intensity might be overestimated

(García+13)

Comparison with other models

XILLVER reflected spectra compared with PEXRAV (Magdziarz & Zdziarski95) for a neutral slab (left panel), and with PEXRIV for an ionized slab (right panel)

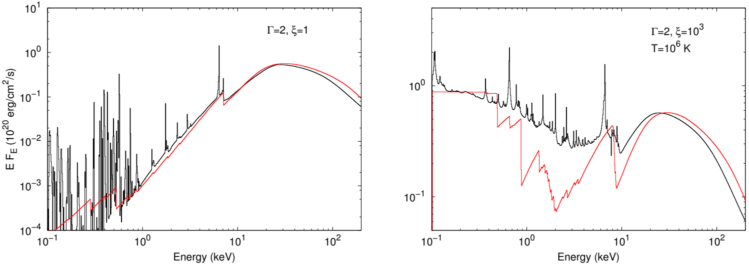

Fits to Observations

Comparison of best-fits to *XMM-Newton* EPIC-pn spectrum of the Circinus galaxy: XILLVER vs. REFLIONX. The lower panels show the data to model ratio for each case. Our model reproduces the Fe Kβ at $\sim$ 7.2 keV and many other features at low-energies.

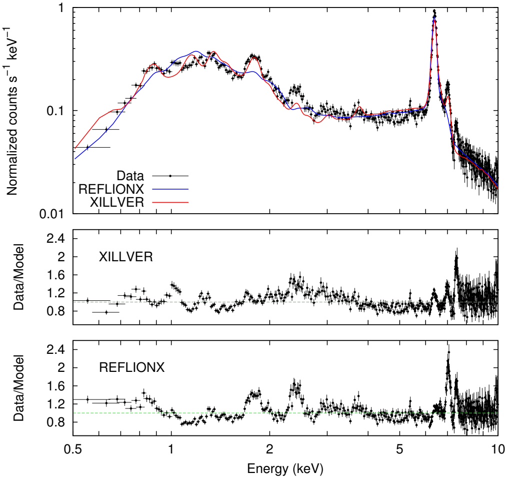

(Kreikenbohm+13)

Variable Photon Index Γ

For large values of ξ (high illumination), the dominant process is the Compton heating and cooling

$$n_e \Gamma_e = \frac{\sigma_{\rm T}}{m_e c^2} \left[\int \varepsilon F_\varepsilon d\varepsilon - 4kT \int F_\varepsilon d\varepsilon \right]$$

In thermodynamic equilibrium, the two terms balance at

$$T_{\rm C} = \frac{\varepsilon}{4k},$$

where $< \varepsilon >= \frac{\int F_\varepsilon \varepsilon d\varepsilon}{F_\varepsilon d\varepsilon}$ is the mean-energy.

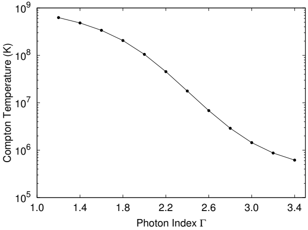

Comparison with other models

XILLVER spectra for $\xi = 10^3$, and REFLIONX for $\xi = 500$. The flux in the continuum at 1 keV differs by ~ 1 order of magnitude.

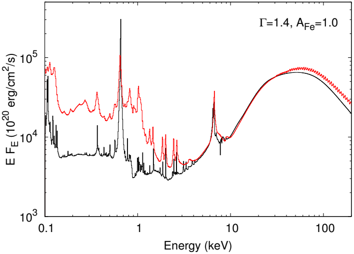

Bremsstrahlung? Comparison with an APEC model for an optically-thin gas at $T = 10^6$ K, $\xi = 10^{-5}$, and a power-law with $\Gamma = 2$.

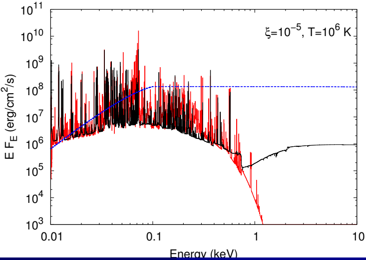

The Compton hump

Comparison of the reflected spectra as calculated with XILLVER, REFLIONX, and the Monte Carlo simulation, for an illumination with $\Gamma = 2$, $\xi = 1$, and solar abundances.

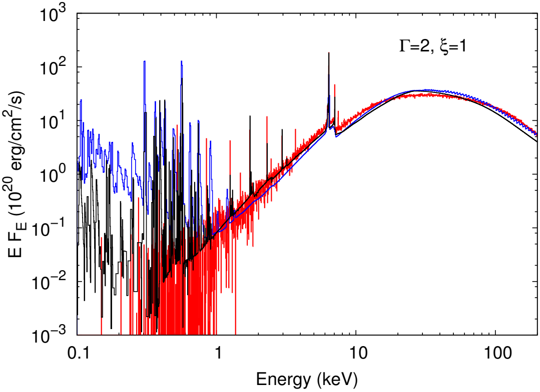

Summary: Broad Emission Line Shapes

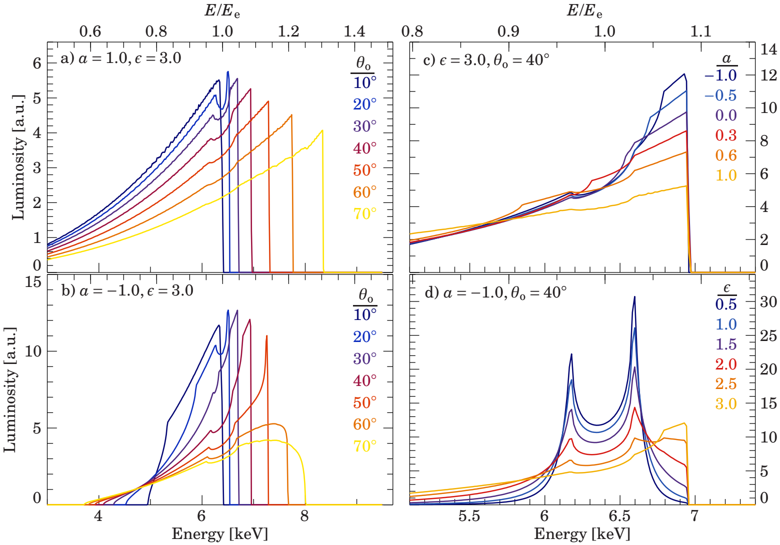

high **Diagnostic Potential** for many parameters

K-shell Photoabsorption

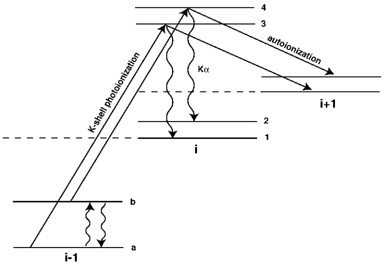

Liedahl+Torres05

The X-ray band ($\sim 0.1 - 10$ keV) covers the emission and absorption produced by the inner-shell transitions of the astrophysically abundant ions (C $\rightarrow$ Ni).

- **Line positions** provide information about the gas composition (identification), as well as about its dynamics (redshifts, gas outflows)
- **Line intensities** provide information about the column of the absorbing material (including ions), constrains on the ionization degree of the gas ($\xi = L/nR^2$), temperature and density
- **Line shapes** provide information about the thermal and turbulent motions of the gas, and can also probe relativistic effects near strong gravitational fields